

Electronic structure and magneto-optical properties of magnetic semiconductors: Europium monochalcogenides

Dipta Bhanu Ghosh, Molly De, and S. K. De

Department of Materials Science, Indian Association for the Cultivation of Science, Jadavpur, Kolkata 700 032, India

(Received 20 February 2004; published 23 September 2004)

Electronic structure and magnetic properties of Europium monochalcogenides (EuX, X=O, S, Se, and Te) have been investigated by the full potential linear muffin-tin orbital method. The generalized gradient approximation (GGA) including on site Coulomb interaction of $5d$ and $4f$ states (GGA+ U_d+U_f) has been used to describe the complicated properties of EuX. The GGA+ U_f band structure underestimates the band gap. GGA+ U_d+U_f gives better agreement in terms of band gap and the positions of $4f$ bands of EuX. GGA+ U_d+U_f gives much improved Kerr spectra for all the EuX over the standard LSDA and GGA+ U_f spectra although the magnitude of the first peak is less satisfactory in the dielectric function spectra. The Coulomb correlation effects among $4f$ and $5d$ electrons of Eu play important role to determine the optical spectra of EuX.

DOI: 10.1103/PhysRevB.70.115211

PACS number(s): 78.20.Ls

I. INTRODUCTION

Among the rare-earth (R) monochalcogenides, Eu monochalcogenides (EuX, X=O, S, Se, and Te) form a very interesting series due to their wide varieties of electronic and magnetic properties. The compounds EuX have NaCl-type crystal structure and the lattice parameters continuously increase from 5.141 Å (EuO) to 6.598 Å (EuTe). The most important feature is that they are magnetic semiconductors which is a very rare combination in R compounds. The experimental electronic energy gaps are 1.12, 1.65, 1.80, and 2.0 eV in EuO, EuS, EuSe, and EuTe, respectively at room temperature.^{1,2} The energy gap can be tuned over a wide energy range (0.334–2.225 eV) by alloying with lead chalcogenides.^{3–5} EuO and EuS are ferromagnetic semiconductors in the ground state. EuSe is a metamagnetic semiconductor with Neel temperature $T_N=4.6$ K. A mixed phase of antiferromagnetic (AFM) and ferrimagnetic ordering appears below 2.8 K. At zero field it becomes MnO-type AFM with $T_N=1.8$ K. Ferromagnetic state exists at high magnetic field.⁶ EuTe is an antiferromagnetic semiconductor at ambient condition and its Neel temperature is $T_N=9.6$ K. The magnetic properties are described by Heisenberg exchange interaction and the magnetization mainly originates from the uncompensated $4f^7$ spin moments of Eu atoms. The exchange interaction between nearest neighbor Eu ions, J_1 and the second nearest neighbor J_2 play important roles in determining the magnetic behavior of EuX along the series.^{7,8} EuO is a ferromagnet with Curie temperature $T_C=69$ K due to the positive values of J_1 and J_2 . The value of J_2 becomes negative for EuS but magnitude is lesser than J_1 which results in ferromagnetic phase of EuS ($T_C=16$ K). The positive value of J_1 decreases sharply while negative value of J_2 becomes stronger in going from oxide to telluride. The competitive values of J_1 and J_2 make the issue about the magnetic phase diagram of EuSe controversial and complicated. The relatively larger negative magnitude of J_2 leads to antiferromagnetic phase of EuTe. The ferromagnetic exchange interaction for all EuX can be enhanced by doping with other rare earth ions such as La, Gd, and Ho (Ref. 9).

The magnetic exchange coupling of $4f$ electrons and the conduction electrons is important due to the localized behavior of $4f$ shell in Eu ions. The temperature dependence of redshift¹⁰ of the optical absorption edge for $4f \rightarrow (5d6s)$ transitions below T_C suggests a strong correlation between the localized magnetic $4f$ state and extended conduction band states. Recently, spin resolved x-ray absorption spectroscopy experiment¹¹ indicates that the redshift is due to the spin splitting of conduction band states. A detailed knowledge about the electronic structure of EuX is necessary to understand the various phenomena. The band structures of EuX have been studied first by Cho¹² using the augmented plane wave (APW) method. Cho observed that $4f$ band positions depend on the type of exchange potential and was able to obtain the actual energy gaps by adjusting the exchange parameters. The $4f$ spin-up states have been dragged down by using preferable values of the exchange parameters. The calculated energy gap of EuO by self-consistent local spin density approximation (LSDA)¹³ is found to be 0.05 eV, much smaller than the experimental one. The temperature dependence of ferromagnetic energy spectrum of EuO (Ref. 14) and EuS (Ref. 15) have been studied by incorporating d - f exchange interaction into the density functional formalism by assuming $4f$ electrons as core states. The structural stability and transitions in EuS, EuSe, and EuTe have been studied¹⁶ within local spin density approximation (LSDA). Most of the studies are concentrated on the change of electronic structures as a function of temperature and pressure. In all these studies correct band gaps of EuX are not obtained due to the two major reasons: (i) failure of density functional theory in semiconductors and (ii) inadequate treatment of strongly correlated $4f$ electrons. The investigations on electronic and magnetic properties should be carried out beyond LSDA.

Magneto-optical (MO) Faraday and Kerr effects are commonly used to investigate the electronic structure as well as magnetic properties of complicated systems. Experimental MO results^{17–19} for all the EuX date back to the 1970's. Faraday rotations are quite large in EuS, EuSe, and EuTe with EuS showing the largest rotation.^{17,19} The experimental Far-

aday rotation spectra are qualitatively similar. However, the Kerr rotation spectrum for EuO differs substantially from that of EuSe (Ref. 17). The temperature variation of the Kerr rotation¹¹ of EuO at an energy of 1.96 eV gives $T_C=69$ K. Faraday rotation calculation²⁰ has been performed for EuS by the LSDA method. It has also been predicted that the complex polar Kerr rotation spectra for EuSe will probably not be reproduced²¹ by the LSDA method. The standard LSDA does not consider the correlated behavior of electrons in the $4f$ shell. The modified LSDA was proposed explicitly including the on site Coulomb interaction $U(\text{LSDA}+U)$ ²² in the conventional model Hamiltonian for the band states. The LSDA+ U provides good description of electronic, magnetic, optical, and magneto-optical properties of Pr mononictides,²³ NdX (Refs. 24 and 25), SmX (Ref. 26) and TmX (Ref. 27). It is our endeavor to find out whether the inclusion of Coulomb interaction in the standard density functional formalism describes the electronic structure and more importantly, the optical and magneto-optical spectra in EuX.

II. CALCULATIONAL DETAILS

Full potential (FP) self-consistent spin-polarized band structure calculations have been performed on EuX by the linear muffin-tin orbital method (LMTO)²⁸ using the FP-LMTO code developed by S. Savrasov *et al.*²⁹ The exchange-correlation potential in the LSDA was calculated with Vosko-Wilk-Nussair parametrization. The improved version of LDA by including the second order gradient correction by Perdew *et al.*³⁰ known as the generalized gradient approximation (GGA) has been used. The density functional theory (DFT) is modified in order to include the strong correlations among the f and d electrons. In the LDA+ U method,^{22,31} the LDA energy functional is modified by removing the LDA f - f interactions and adding the strong on-site Coulomb interactions among the f electrons. The details of the calculation of the correlation part is given in our previous paper.²³ This idea is adopted and extended for d - d interactions also. The need for such a formalism arose due to the presence of $5d$ state in valence band in LSDA/GGA calculations and the possibility that this occupied part of the $5d$ state may be correlated. This aspect is discussed in more detail later in the paper.

The value of $F^0(=U_d$ and $U_f)$ is chosen as parameter and varied between 2.5–14 eV for studying the effects of correlation on the electronic as well as magneto-optical properties of EuX. The values of other Slater integrals F^2 , F^4 for the d electrons and F^2 , F^4 , F^6 for the f electrons used are 0.8 times of their atomic values evaluated within Hartree-Fock (HF) approximation³² in order to calculate the Coulomb and exchange matrices $U_{mm'}$ and $J_{mm'}$. The experimental¹ lattice parameters with rock-salt-type structure at ambient conditions for EuX are given in Table I and it also provides muffin-tin radii of Eu and the chalcogen atom used in the calculations. The basis consists of Eu $6s$, $5p$, $5d$, $4f$, and chalcogen $(n)s$, $(n)p$, and $(n)d$, where n refers to the principal quantum number. The $5s$ electrons of Eu and $(n-1)d$ electrons of Se and Te were treated in a separate panel and

TABLE I. Table contains a , the lattice parameter, muffin-tin radii of Eu, S_{Eu} and chalcogen (X), S_X , correlation values for d , U_d and that for f states, U_f and the corresponding calculated and experimental energy gap, E_g^{cal} and E_g^{expt} , respectively.

	a (a.u.)	S_{Eu} (a.u.)	S_X (a.u.)	U_d (eV)	U_f (eV)	E_g^{cal} (eV)	E_g^{expt} (eV)
EuO	9.715	2.866	1.992	5.0	5.0	1.03	1.12
EuS	11.278	3.044	2.593	8.0	4.0	1.56	1.65
EuSe	11.707	3.102	2.751	8.0	3.5	1.62	1.80
EuTe	12.468	3.179	3.055	12.0	2.5	1.78	2.00

hence were not included in the optical calculations. Charge density, density of states and the momentum matrix elements were calculated on a grid of 242 \mathbf{k} points in irreducible Brillouin zone and the \mathbf{k} space integration was performed using the tetrahedron method. All of the seven $4f$ spin-up states have been considered as fully occupied states. The magnetic transition temperatures in EuSe and EuTe are very low. Hence we performed FP spin-polarized ferromagnetic calculations on the EuX. Simple LSDA calculations on all the EuX have also been performed for the sake of comparison.

III. RESULTS AND DISCUSSION

The LSDA band structures show the presence of mostly localized f bands of Eu in the vicinity of Fermi level, E_F and wide $5d$ bands of Eu fill up the bottom of the conduction band. Hence, it is seen that LSDA calculations do not produce any kind of direct or indirect energy gap for any of the EuX which contradicts the experimental observation that they are magnetic semiconductors. The inclusion of correlation effect of f states (U_f) splits the occupied and unoccupied f bands and consequently gives rise to an energy gap around E_F . The indirect gap in EuO has been calculated from the energy difference between the top of the valence f band at Γ point and the bottom of the conduction d band at the X point. The direct band gap at the X point is almost the same as that of indirect gap. The value of U_f for the elemental Eu atom is about 11 eV as obtained from XPS and BIS experiments.³³ The value of U_f was tuned in the entire range but this neither gave the proper gap nor a satisfactory band structure. Though the gap for $U_f=9$ eV of 1.15 eV reaches very close to the experiments, the energetic positions of the $4f$ and chalcogen p band, below E_F , are rather poor in comparison.

Similar GGA+ $U_f(=9$ eV) calculation in EuSe gives a gap of 1.37 eV which is comparable to the experimental one of 1.8 eV. But the occupied f states of Eu are pushed away from the Fermi level and p band of Se occupy the top of the valence band which is not the order in the experimental spectra. This trend is also followed in EuTe and ends up in a drastic reduction of band gap to 0.8 eV.

The incorporation of U_f influences only f states. Quite predictably, we find that increasing the magnitude of U_f does not lead to the actual band gap of EuTe. The energy gap in all the EuX is formed between $4f$ and $5d$ bands of Eu. The magnetic properties of EuX are described by the indirect and

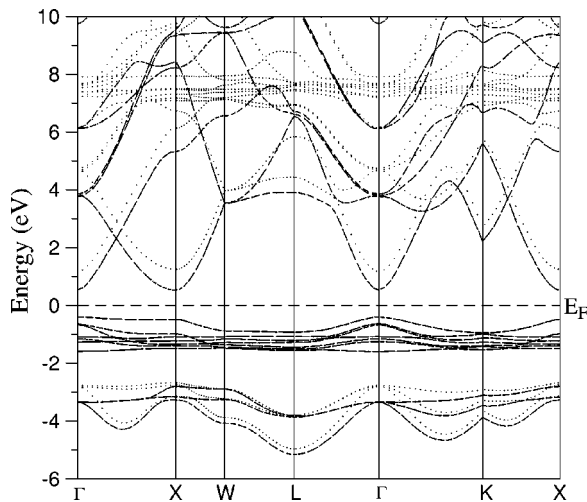


FIG. 1. Band structure of EuO in the FM phase.

super-exchange interactions between f and $5d$ orbitals of Eu. The temperature variation of optical absorption spectra are explained by the spin splitting of $5d$ states induced by the localized $4f$ spins. The GGA+ U_f calculations indicate that a strong hybridization exists between $4f$ and $5d$ states. Thus a part of $5d$ orbitals are occupied and consequently appear in valence band region. These facts stimulated us to take into account the correlation effects of $5d$ electrons too. The gaps calculated, by considering the on-site Coulomb interactions of $5d$ electrons along with that of the $4f$ electrons, are remarkably in good agreement with the experimental results as shown in Table I. The valence band is the admixture of p states of chalcogen and $5d$ and $4f$ states of Eu. The energetic positions of $4f$ bands are determined by proper choice of U_f . The bottom of the conduction band is the $5d$ character of Eu. The inclusion of Coulomb interaction in $5d$ states mainly changes the bottom of the conduction band by upward energy shifting from original position due to Hubbard U_d . As a consequence the energy gap improves and becomes comparable with the experimental value. In LDA+ U scheme, the on-site Coulomb interaction is effective when U is large compared to bandwidth. The splitting between lower and upper Hubbard bands depend on the orbital occupancies. The larger bandwidth and smaller occupation numbers of $5d$ states compared to $4f$ states result in larger values of U_d than U_f .

The self-consistent band structure of EuO within GGA+ U_d+U_f ($U_d=5$ eV and $U_f=5$ eV) formalism is shown in Fig. 1. The chosen U_d and U_f values are not arbitrary but are optimized so as to reach closer to experiments. The optimized U_d and U_f values along with their corresponding gaps are shown in Table I. Also a set of U_d and U_f values along with their corresponding gaps for the series are printed in Table II. The occupied seven $4f$ bands appear between the p bands of O and the conduction bands, and the O p bands are well separated from the Eu f bands. The conduction band consists of the unoccupied Eu f and Eu d hybridized bands. The band structures of the remaining EuX, not shown here, are quite similar except for the separation and position of

TABLE II. Table contains comparison of band gaps for different correlation values for the EuX.

	U_d (eV)	U_f (eV)	E_g (eV)		U_d (eV)	U_f (eV)	E_g (eV)
EuO	0.0	8.0	0.87	EuSe	7.5	3.0	1.374
	0.0	9.0	1.15		8.0	3.5	1.620
	5.0	5.0	1.03		10.0	2.5	1.59
	6.0	5.0	1.21		10.0	3.5	1.90
	10.0	5.5	1.33		11.0	3.5	1.986
EuS	8.0	4.0	1.56	EuTe	10.0	3.0	1.455
	10.0	3.0	1.36		12.0	2.5	1.782
					14.0	3.0	2.027

occupied and unoccupied Eu f states and the separation between the valence Eu f and chalcogen p states. The energy level of the $6s$ state at Γ point is almost the same as that of the $5d$ state at the X point in all the EuX. There is no direct experimental evidence for this nearly same level of $6s$ and $5d$ states. Mobility of conduction electrons from Hall measurements³⁴ only suggests that there may be significant contribution from $6s$ states. This is also predicted by Kasuya in exciton model³⁵ in order to interpret the anomalous transport properties of EuX.

The angular momentum decomposed density of states (DOS) for all the Eu monochalcogenides are shown in Fig. 2. The spin-decomposed density of states in EuO above E_f (see inset) show substantial agreement with the spin resolved unoccupied oxygen p states as obtained from the spin-resolved x-ray absorption spectroscopy.¹¹ The energy gap gradually

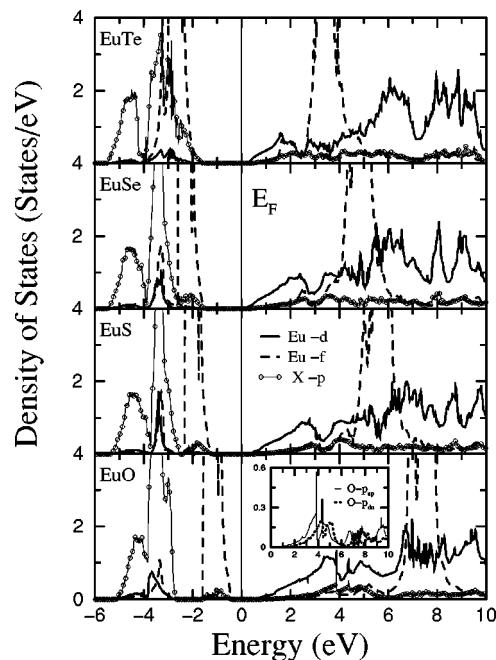
FIG. 2. l -projected density of states of Eu monochalcogenides. Inset shows the spin-resolved unoccupied oxygen p states in EuO.

TABLE III. Table contains m_s and m_0 , the atomic orbital and spin moments, respectively, and the total moment m_s+m_0 .

	$m_s(\text{Eu})$	$m_s(X)$	$m_0(\text{Eu})$	$m_0(X)$	m_s+m_0
	μ_B	μ_B	μ_B	μ_B	μ_B
EuO	6.788	-0.058	0.070	0.000	6.800
EuS	6.785	-0.030	0.076	0.000	6.831
EuSe	6.791	-0.028	0.078	0.000	6.841
EuTe	6.790	-0.020	0.080	0.000	6.850

increases from EuO to EuTe which is evident from this figure. The partial DOS reveals that the position of occupied f bands shifts away from E_F and the spin-orbit splitting of the p bands increases with the increase in atomic number of chalcogen. This is in agreement with the experimental photo emission results.³⁶ The gradual shifting of f bands away from E_F with the increasing chalcogen atomic number results in p - f mixing in EuSe and EuTe and is stronger in the latter. The top of the valence band is the $4f$ band and the bottom of the conduction band is the d state for all EuX.

Table III contains the spin and the orbital moments of Eu and the chalcogen atoms along with the total moment. All the EuX exhibit large spin polarization, most of which is due to spin polarization of the f states of the Eu atom. Orbital moment is negligible in all the chalcogenides. Hence, we find that spin splitting of the f states of the Eu atom solely contribute to the magnetic properties of the EuX. The calculated magnetic moment given in Table III is consistent with half filled f^7 S state ion ($L=0, J=S=7/2$) with spin $7/2$ and negligible orbital moment.

The comprehensive studies about the effect of correlations among the d and f states on the gaps of EuX as shown in Table II are performed. The values of U_d and U_f as shown in Table I are used for the reasonable electronic structure of EuX. All other combinations of U_d and U_f values lead to less satisfactory band gaps and/or band structure. The most interesting property of EuX materials is that EuO and EuS exhibit metal-insulator transition and large magnetoresistance around T_C in Eu rich samples.³⁷ Similar behavior has also been found in strongly correlated transition metal oxides $\text{La}_{(1-x)}\text{Ca}_x\text{MnO}_3$. Satpathy *et al.*³⁸ studied the electronic structure taking into account the correlation effects of d states of Mn (LSDA+ U technique). They found that magnetic insulating states of LaMnO_3 and CaMnO_3 appeared for $U \approx 10$ eV. The magnetic semiconducting ground state of EuX is also obtained by varying U_d from 5 to 12 eV along the series of EuX. The present calculation indicates that there is a strong resemblance between these two classes of materials.

The optical properties of solids can be described by the complex dielectric function $\epsilon(\omega) = \epsilon_1(\omega) + i\epsilon_2(\omega)$. The LMTO calculations provide the imaginary component of the diagonal element and the real component of the off-diagonal element of the dielectric function which are calculated from the electronic structure using the following relation:

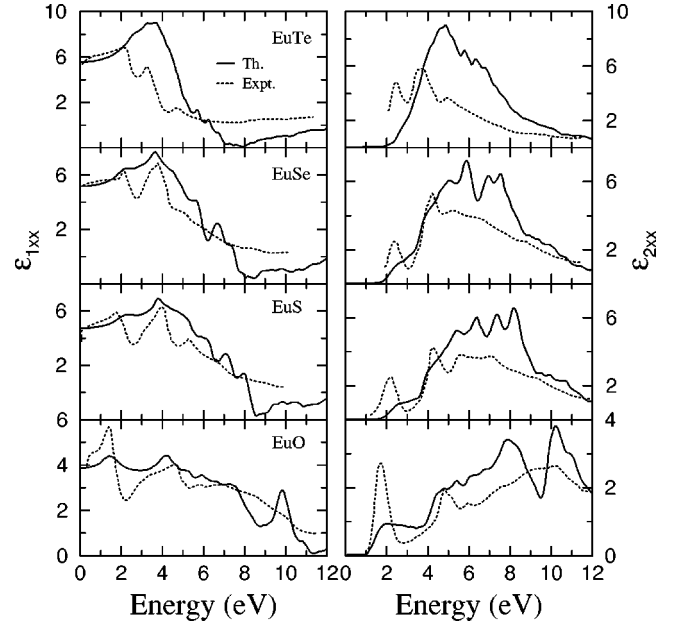


FIG. 3. Calculated real diagonal (left panel) part and imaginary diagonal (right panel) part of dielectric function of Eu monochalcogenides and their corresponding experimental (Ref. 18) spectrum.

$$\epsilon_{ij}(\omega) = \frac{4\pi^2 e^2}{\Omega m^2 \omega^2} \sum_{\mathbf{k}n\mathbf{n}'\sigma} \langle \mathbf{k}n\sigma | p_i | \mathbf{k}n'\sigma \rangle \langle \mathbf{k}n'\sigma | p_j | \mathbf{k}n\sigma \rangle \times f_{\mathbf{k}n}(1 - f_{\mathbf{k}n'}) \delta(e_{\mathbf{k}n'} - e_{\mathbf{k}n} - \hbar\omega), \quad (1)$$

where Ω is the volume, σ is the spin index, e is the electronic charge, and m its mass. The conductivity $\sigma_{ij}(\omega)$ is obtained from

$$\epsilon_{ij}(\omega) = \delta_{ij} + i \frac{4\pi}{\omega} \sigma_{ij}(\omega). \quad (2)$$

The imaginary component of diagonal optical conductivity (σ_{xx}^2) and the real component of off-diagonal conductivity (σ_{xy}^1) have been calculated using the Kramers-Kronig (KK) transformation. Optical and magneto-optical spectra have been calculated for all the EuX using the FP-LMTO band structure. Furthermore, a Lorentzian broadening of about 0.068 eV has been used in order to obtain the best agreement with the experimental results.

Left panel of Fig. 3 shows the calculated (GGA+ U_d + U_f) and experimental real diagonal component of the dielectric function, $\epsilon_{1xx}(\omega)$ for all the EuX. It is obtained from KK transformation of the calculated (GGA+ U_d + U_f) imaginary component of the diagonal dielectric function $\epsilon_{2xx}(\omega)$. The latter and its experimental counterpart for all the EuX are shown in the right panel of Fig. 3. The experimental ϵ_{2xx} spectra exhibit two peaks in the energy range of 1–5 eV and small structures between 6–10 eV. The first experimental peak at about 1.75 eV of the absorption spectra for EuO is very sharp. The origin of small width is generally described by the formation of multiplet structures arising from the spin-orbit coupling in the excited $4f^6$ states.^{35,39,40} The calculated spectra do not reproduce experimental sharp peak

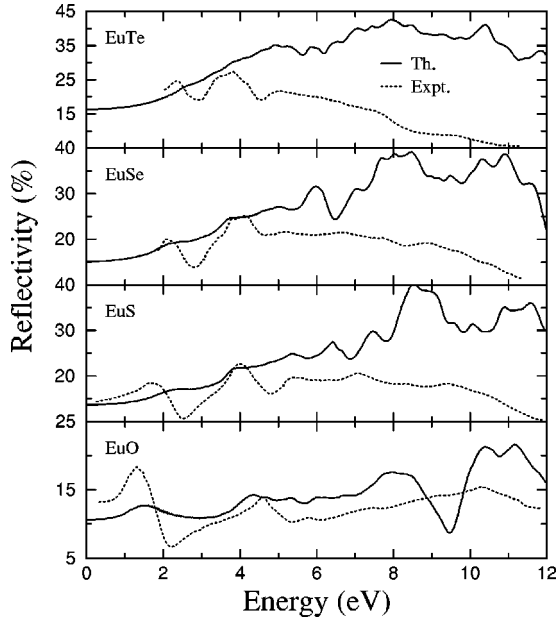


FIG. 4. Calculated and experimental (Ref. 18) reflectivity spectra of Eu monochalcogenides.

around 1.75 eV. This deficiency occurs because the first peak is essentially due to magnetic exciton but with a small inter-band transition contribution. The first relatively broader optical absorption structure, in the calculated spectra, at about 1.9 eV is due to transitions from the lower Hubbard $4f$ band to the $5d$ bands of Eu above E_F . The multiplet structures smear out due to formation of the $5d$ band which gives the broad peak. The second experimental peak at 4.8 eV is attributed to transitions from Eu f to spin-split $5d$ states of Eu. In the calculated spectra this structure along with the first one are suppressed due to the underestimated splitting of the $5d$ band in the conduction band. A small absorption attributed to $p \rightarrow d$ transitions starts from 3.5 eV for EuO in the experimental spectrum. This feature is not evident in the calculated spectrum due to significant contribution of $4f \rightarrow 5d$ transitions. Hence theoretical absorption spectra are much broader and found at higher energy.

The agreement with the experimental spectra is substantial in all EuX but EuTe, where the peaks become indistinguishable. In EuTe, two experimental peaks are seen whereas they are bunched together in the calculated spectra. The lowest structure due to $f \rightarrow d$ transition occurs at an energy higher than the corresponding experimental structure. This is suppressed due to transitions from the wide p - f hybridized band to $5d$ bands occurring at a slightly higher energy. This anomaly could only be removed by suitably choosing U_f and U_d such that the lower Hubbard f band has a smaller hybridization with the Te p states. But this method of tuning fails and leads to an underestimation of band gap and inappropriate band structure in EuTe. The theoretical spectra show structures at low energy while prominent peaks at higher energy. The distinct peaks appear at lower energy as X changes from Te to O. Largely, the theoretical spectra follow the experimental ones.

$\epsilon_{1xx}(0)$ is about 4.0 for EuO and the spectrum stays dispersionless for ω less than or equal to the band gap. This

spectrum, $\epsilon_{1xx}(\omega)$ (left panel of Fig. 3) reveals a resonant structure wherever $\epsilon_{2xx}(\omega)$ shows an absorption. At higher energy, ϵ_{1xx} deviates from the experimental results and becomes negative.

Reflectivity is calculated from the relation

$$R(\omega) = \left| \frac{\sqrt{\epsilon_{xx}(\omega)} - 1}{\sqrt{\epsilon_{xx}(\omega)} + 1} \right|^2. \quad (3)$$

Calculated GGA+ U_d+U_f and experimental reflectivity spectra of EuX are shown in Fig. 4. Reflectivity shows a gradual increase in its absolute value as X is changed from oxygen to tellurium. This is true for the experimental spectrum, too. Experimentally, in EuO, the height of first peak at about 1.3 eV is more than the second one at about 4.6 eV which is not so in the theoretical spectra, although the positions of the peaks are well agreed with experiments. Systematic studies on the reflectivity spectra of $\text{Eu}_{1-x}\text{Sr}_x\text{S}$ for the composition range $x=0$ to 1 indicates that the excitation peaks around 4 eV are due to p to d transitions at the X point.⁴¹ A prominent structure around 4 eV is observed in the calculated spectra for EuS. This arises due to the combination of $p \rightarrow d$ and $f \rightarrow d$ transitions. For EuTe there are no distinct peaks at lower energy in the theoretical spectra due to reasons discussed above.

Magneto-optical Kerr rotation is calculated from the relation

$$\Phi_k = \theta_k(\omega) + i\epsilon_k(\omega) \approx \frac{-\sigma_{xy}}{\sigma_{xx} \sqrt{1 + \frac{4\pi i}{\omega} \sigma_{xx}}}. \quad (4)$$

Magneto-optical Faraday rotation per unit thickness is given by the relation

$$\Phi_F = \theta_F(\omega) + i\epsilon_F(\omega) \approx \frac{\sigma_{xy}}{\sqrt{1 + \frac{4\pi i}{\omega} \sigma_{xx}}} \frac{2\pi}{c}, \quad (5)$$

where σ_{xx} and σ_{xy} are the diagonal and off-diagonal components of the optical conductivity tensor, provided both are small and $|\sigma_{xy}| \ll |\sigma_{xx}|$. Here θ_k and ϵ_k are Kerr rotation and Kerr ellipticity, respectively. θ_F and ϵ_F are Faraday rotation and magnetic circular dichroism, respectively. Velocity of light is represented by c .

Left and right panel of Fig. 5 depict the LSDA (for EuO only), GGA+ U_d+U_f and their corresponding experimental Kerr rotation and the ellipticity spectra of EuX, respectively. LSDA calculations on EuO shows a large rotation of about -7° at about 0.5 eV while it appears at 1.4 eV in experiment. GGA+ U_d+U_f calculation gives a rotation of about -2.3° at 1.6 eV. In general the magnitude of positive rotation is smaller for the theoretical calculations and found at a higher energy compared to experiment. The experimental double structure in ellipticity of EuO is much narrower than the theoretically predicted ones which indicates that the $4f^7$ state is much more localized than the calculated ones. This inadequacy leads to the peaks due to $f \rightarrow d$ transitions in the GGA+ U_d+U_f spectra being broader than the experimental peaks. The magnitude of the first Kerr rotation goes on de-

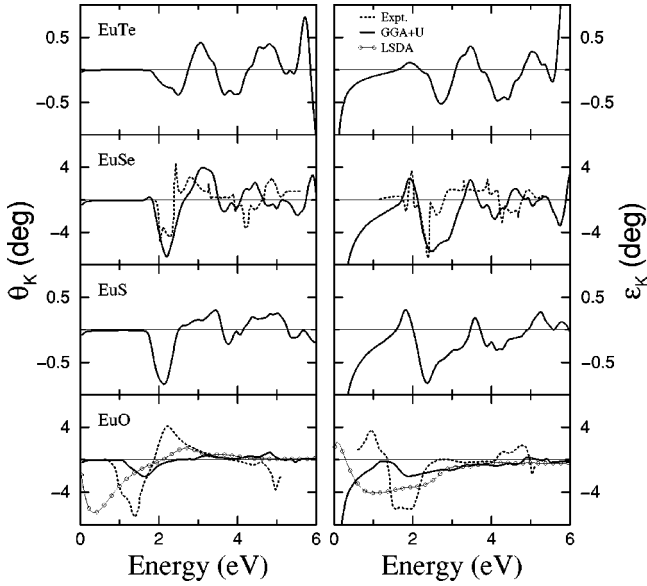


FIG. 5. Calculated and experimental (Ref. 19) polar Kerr rotation (left panel) and Kerr ellipticity (right panel) spectra of Eu monochalcogenides (in the case of EuSe the calculated spectra are multiplied by a factor of 10).

creasing as one moves to the higher chalcogenide. The calculated spectra of EuSe differ in magnitude with its experimental counterpart by an order. In spite of this difference the nature and energetic positions of the spectral features are comparable with the measured ones.

GGA+ U_d+U_f calculated Faraday rotation and magnetic circular dichroism for all the Eu monochalcogenides, along with the experimental Faraday rotation spectra for EuS, EuSe, and EuTe are shown in left and right panels of Fig. 6, respectively. EuO gives the maximum Faraday rotation of about 0.35×10^6 deg./cm at about 1.85 eV. No experimental data is available on the Faraday rotation of EuO. For EuS the

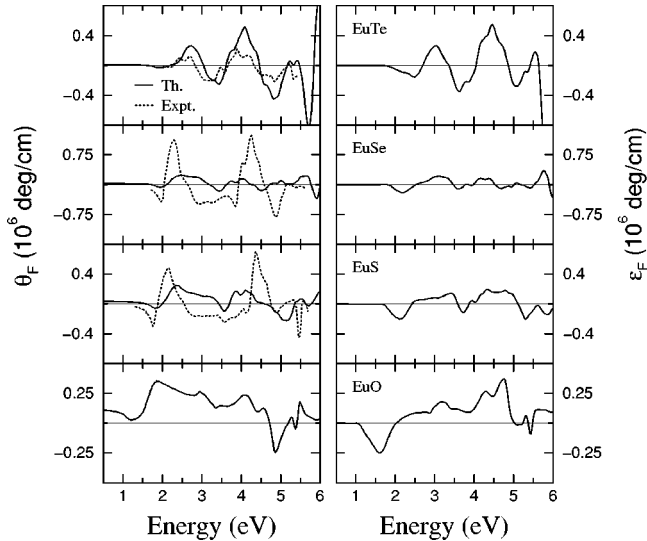


FIG. 6. Left panel: calculated and experimental (Ref. 19) Faraday rotation spectra of Eu monochalcogenides. Right panel: calculated Faraday ellipticity spectra of Eu monochalcogenides.

first positive peak of magnitude 0.25×10^6 deg./cm at about 2.35 eV corresponds to the experimental one at 2.1 eV of magnitude 0.45×10^6 deg./cm. Experimentally, EuS shows the largest rotation of about 0.7×10^6 deg./cm at about 4.35 eV, which can be compared with the theoretical double structure around 4 eV. This trend is also present in EuSe spectra. However, in the case of EuTe, there is excellent correspondence with the experiment except for the first experimental double structure around 2.5 eV, which is a broad peak in the calculated spectra. This is surprising if we consider the discrepancy between the calculated and experimental diagonal dielectric function. This proves that the magneto-optical effect is a phenomenon governed by the interplay between spin polarization and spin-orbit splitting. The off-diagonal conductivity contains these interactions and appears in magneto-optical spectra. Optical properties which are not dependent upon the off-diagonal elements, such as the dielectric function, are mainly influenced by the joint density of states and the transition probabilities. These two factors are of less importance in determining the magneto-optical behavior of Eu monochalcogenides and hence magneto-optical Faraday rotation spectra show better agreement with the experiment.

The optical and magneto-optical spectra of EuX are complex due to the various interactions of $5d$ excited states with the surroundings. Different theoretical models based on spin-orbit coupling, spin-flip transitions, magnetic exciton, and localized magnetic polaron exist. Sharp peaks originate from the multiplet structures of localized $4f^6$ states.³⁹ The creation of the localized magnetic polaron and the large lattice relaxation around the $4f$ hole are cited to be necessary for explaining the characteristics of the temperature-dependent luminescence spectra.^{42–45} The optical spectra are qualitatively explained by the magnetic exciton model.^{35,46} In this scheme an electron from the $4f^7$ state is excited to $5d$ state and is bound through Coulomb interaction between the electron and the $4f$ hole. The excited electron interacts with localized $4f^7$ spins via d - f exchange interaction. As a result of it the excited electron enhances the exchange splitting due to the formation of excess local magnetization. The bottom of the $5d$ conduction band (absorption) edge is formed by the magnetic exciton which reduces the effect of band formation of $5d$ excited states. The optical and magneto-optical data are due to the combination of magnetic exciton and interband transitions. The subtraction of the magnetic exciton effect from the observed data in one particle band calculation is difficult as it is associated with the interband transitions. Hence the disagreement in magnitude and the overall discrepancy in the spectra may be due to the lesser degree of localization of the occupied f states, weak effect of the crystal-field splitting of the $5d$ states of Eu, exclusion of the d - f exchange interaction and magnetic excitonic effect in our calculation. However, the present calculation suggests that on-site Coulomb interaction is also important in addition to other effects.

IV. CONCLUSION

We report the inclusion of d states as the correlated ones along with the f states in the band structure calculations. This

inclusion estimates correct indirect energy gaps for EuX. The calculations suggest an ascending value of Coulomb interaction parameter for the d states and descending one for the f states as one moves from EuO to EuTe in order to obtain the correct valence band structure at least. The same calculations provide neck comparison with experiment in different optical and magneto-optical behaviors up to the energy of 6 eV. At higher energy the comparison is rather poor which is a general failure of the density functional method. The present calculations give an indepth view on the electronic structure of the EuX. The optical and the magneto-optical properties show better agreement when calculated with this

method. The satisfactory agreement in optical spectra suggest that both $4f$ and $5d$ states are correlated. Orbital polarization is negligible here. Magnetic excitonic effects and spin-flip transitions may minimize the disagreement between the theoretical and experimental results that still exist.

ACKNOWLEDGMENT

This work is funded by the Department of Science and Technology, Government of India (Project No. SP/S2/M-50/98).

- ¹A. Jayaraman, A. K. Singh, A. Chatterjee, and S. Usha Devi, Phys. Rev. B **9**, 2513 (1974).
- ²A. Mauger and C. Godart, Phys. Rep. **141**, 51 (1986).
- ³D. U. Bartholomew, J. K. Furdyna, and A. K. Ramdas, Phys. Rev. B **34**, 6943 (1986).
- ⁴Heinz Krenn, Shu Yuan, Norbert Frank, and Gunther Bauer, Phys. Rev. B **57**, 2393 (1997).
- ⁵H. Krenn, W. Herbst, H. Pascher, Y. Ueta, G. Springholz, and G. Bauer, Phys. Rev. B **60**, 8117 (1999).
- ⁶R. Griessen, M. Landolt, and H. R. Ott, Solid State Commun. **9**, 2219 (1971).
- ⁷L. Passell, O. W. Dietrich, and J. Als-Nielsen, Phys. Rev. B **14**, 4897 (1976).
- ⁸H. G. Bohn, W. Zinn, B. Dorner, and A. Kollmar, Phys. Rev. B **22**, 5447 (1980).
- ⁹J. Vitins and P. Wachter, Phys. Rev. B **12**, 3829 (1975).
- ¹⁰B. Batlogg, E. Kaldis, A. Schlegel, and P. Wachter, Phys. Rev. B **12**, 3940 (1975).
- ¹¹P. G. Steeneken, L. H. Tjeng, I. Elfimov, G. A. Sawatzky, G. Ghiringhelli, N. B. Brookes, and D. J. Huang, Phys. Rev. Lett. **88**, 047201 (2002).
- ¹²S. J. Cho, Phys. Rev. B **1**, 4589 (1970).
- ¹³P. M. Oppeneer and V. N. Antonov, *Spin-Orbit-Influenced Spectroscopies of Magnetic Solids*, edited by H. Ebert and G. Schutz (Springer, Berlin, 1996), p. 29.
- ¹⁴R. Schiller and W. Nolting, Solid State Commun. **118**, 173 (2001).
- ¹⁵W. Muller and W. Nolting, Phys. Rev. B **66**, 085205 (2002).
- ¹⁶D. Singh, V. Srivastava, M. Rajagopalan, M. Husain, and A. K. Bandyopadhyay, Phys. Rev. B **64**, 115110 (2001); D. Singh, M. Rajagopalan, and A. K. Bandyopadhyay, Solid State Commun. **112**, 39 (1999); D. Singh, M. Rajagopalan, M. Husain, and A. K. Bandyopadhyay, *ibid.* **115**, 323 (2000).
- ¹⁷W. Reim and J. Schoenes, in *Ferromagnetic Materials*, edited by E. P. Wohlfarth, and K. H. J. Buschow (North Holland, Amsterdam, 1990), Vol. 5, p. 133.
- ¹⁸G. Güntherodt, Phys. Cond. Matter **18**, 37 (1974).
- ¹⁹J. Schoenes, Z. Phys. B **20**, 345 (1975).
- ²⁰Y. A. Uspenskii, E. T. Kulatov, and S. V. Halilov, Physica A **241**, 89 (1997).
- ²¹P. M. Oppeneer, *Handbook of Magnetic Materials*, edited by K. H. J. Buschow (Elsevier Science, Amsterdam, 2001), Vol. 13.
- ²²V. I. Anisimov, J. Zaanen, and O. K. Andersen, Phys. Rev. B **44**, 943 (1991).
- ²³D. B. Ghosh, M. De, and S. K. De, Phys. Rev. B **67**, 035118 (2003).
- ²⁴V. N. Antonov, B. N. Harmon, A. Ya. Parlov, and A. N. Yaresko, Phys. Rev. B **59**, 14 561 (1999).
- ²⁵M. De, and S. K. De, J. Phys.: Condens. Matter **11**, 6277 (1999).
- ²⁶V. N. Antonov, B. N. Harmon, and A. N. Yaresko, Phys. Rev. B **66**, 165208 (2002).
- ²⁷V. N. Antonov, B. N. Harmon, and A. N. Yaresko, Phys. Rev. B **63**, 205112 (2001).
- ²⁸O. K. Andersen, Phys. Rev. B **12**, 3060 (1975).
- ²⁹S. Y. Savrasov and D. Y. Savrasov, Phys. Rev. B **46**, 12 181 (1992); S. Y. Savrasov, *ibid.* **54**, 16 470 (1996).
- ³⁰J. P. Perdew, K. Burke, and Y. Wang, Phys. Rev. B **54**, 16 533 (1996).
- ³¹V. I. Anisimov, F. Aryasetiawan, and A. I. Lichtenstein, J. Phys.: Condens. Matter **9**, 767 (1997).
- ³²R. D. Cowan, *The Theory of Atomic Structure and Spectra* (University of California Press, Berkley 1981).
- ³³J. K. Lang, Y. Baer, and P. A. Cox, J. Phys. F: Met. Phys. **11**, 12 (1981).
- ³⁴S. Von Molnar and S. Methfessel, J. Appl. Phys. **38**, 959 (1967).
- ³⁵T. Kasuya and A. Yanase, Rev. Mod. Phys. **40**, 684 (1968).
- ³⁶D. E. Eastman, F. Holzberg, and S. Methfessel, Phys. Rev. Lett. **23**, 226 (1969).
- ³⁷E. L. Nagaev, Phys. Rep. **346**, 387 (2001).
- ³⁸S. Satpathy, Zoran S. Popovic, and Filip R. Vukajlovic, Phys. Rev. Lett. **76**, 960 (1996).
- ³⁹O. Sakai, A. Yanase, and T. Kasuya, J. Phys. Soc. Jpn. **42**, 596 (1977).
- ⁴⁰M. Freiser, S. Methfessel, and F. Holtzberg, J. Appl. Phys. **39**, 900 (1968).
- ⁴¹Y. Kaneko, T. Mitani, and T. Koda, J. Phys. Soc. Jpn. **47**, 1029 (1979).
- ⁴²M. Umehara, J. Magn. Magn. Mater. **187**, 177 (1998).
- ⁴³R. Akimoto, M. Kobayashi, and T. Suzuki, J. Phys. Soc. Jpn. **63**, 4616 (1994).
- ⁴⁴M. Umehara, Phys. Rev. B **65**, 205208 (2002).
- ⁴⁵P. Wachter, CRC Crit. Rev. Solid State Sci. **3**, 189 (1972).
- ⁴⁶T. Kasuya, CRC Crit. Rev. Solid State Sci. **3**, 131 (1972).